Experimental observation of the steady – oscillatory transition in a cubic lid-driven cavity

A. Liberzon, Yu. Feldman and A. Yu. Gelfgat

School of Mechanical Engineering, Faculty of Engineering, Tel-Aviv University, Ramat Aviv, 69978, Tel-Aviv, Israel

Abstract

Particle image velocimetry is applied to the lid-driven flow in a cube to validate the numerical prediction of steady – oscillatory transition at lower than ever observed Reynolds number. Experimental results agree with the numerical simulation demonstrating large amplitude oscillatory motion overlaying the base quasi-two-dimensional flow in the mid-plane. A good agreement in the values of critical Reynolds number and frequency of the appearing oscillations, as well as similar spatial distributions of the oscillations amplitude are obtained.

I. INTRODUCTION

Accurate prediction of the flow conditions in the driven cavity is of outmost importance for a number of technological applications, such as coating and polishing processes in microelectronics, passive and active flow control using blowing/suction cavities and riblets[1]. Moreover, citing Shankar and Deshpande[1], "…the overwhelming importance of these flows is to the basic study of fluid dynamics". The driven cavity flow has well defined boundary conditions and it is apparently straightforward to use this configuration for benchmarking of numerical and experimental studies of fluid flows. Moreover, it can be shown that upon geometrical similarity (the width to height and width to span ratios) a single dimensionless number describes the flow state, namely the Reynolds number. Typically it is based on the cavity length, L and the driving lid velocity, U. The fixed flow domain makes this flow attractive also for experimental purposes, in particular, for studying flow transitions at large Reynolds numbers. Though

apparently simple, the lid-driven cavity flows exhibit a vast variety of flow patterns, from 2D to 3D, secondary, corner and streamwise eddies, chaotic trajectories and more.

Despite the extensive research effort and very accurate numerical description of the two-dimension lid-driven cavity flow, the prediction of properties of corresponding three-dimensional flows for a given cavity geometry and at a given Reynolds number is still elusive. For example, the critical Reynolds number for a primary flow bifurcation was reported to be below 6000 (e.g. Ref.[1] and references therein). Bogatyrev & Gorin[2] and later Koseff & Street[3] experimentally observed 3-D unsteady flows at much lower Reynolds numbers, being close to 3000 in a cubical cavity. The observation was then verified by a more recent numerical study of Iwatsu et al.[4] who predicted an instability onset at the range of $2000 < Re < 3000$. Thus, Figure 20a in Shankar and Deshpande[1], shows oscillations of velocity close to the wall of a cubical cavity, measured at $Re = 3200$ by Prasad and Koseff.[5] The authors, however, did not pursue this research to identify the lowest Reynolds number at which the large amplitude fluctuations are observable. Very recently we (Feldman and Gelfgat[6]) reported rather accurate time-dependent computations of a 3D cubical lid-driven cavity flow, in which the steady – oscillatory transition was found to take place at even lower Reynolds number of approximately 1900. In order to validate these numerical results we conducted a series of experiments in a cubical cavity that was used for the Lagrangian tracking (Krezier et al.[7]). We report here on the very good qualitative and quantitative agreement between the numerical and experimental results.

The experimental setup is briefly described in the following Section II, for the sake of completeness. We proceed to the main results in Section III, comparing the flow before and after the steady oscillatory transition, namely at the Reynolds numbers of 1480 and 1970. We present flow snapshots, describe in details the unstable modes and give some conclusive remarks in Section IV.

II. EXPERIMENTAL SET UP

Experiments are performed in a cubical with a side length L =80 mm, whose upper boundary moves with a constant velocity U in the x direction as shown in Figure 1-a. All other cavity boundaries are stationary. The cavity is filled with a tap water and its moving

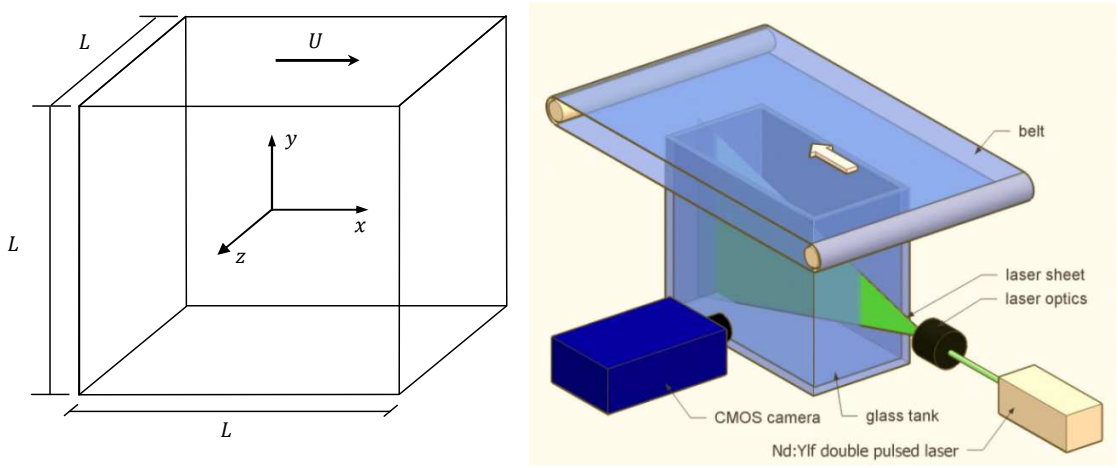

(a) (b)

FIG. 1. Lid driven cavity: (a) physical model and coordinate system ;(b) sketch of the experimental set up.

lid comprises a circularly closed plastic belt driven by a DC motor. The particle image velocimetry (PIV) technique was used for the flow measurements. The experimental setup is shown schematically in Figure 1-b. A more detailed description including hardware and software components for data acquisition and processing, as well as estimated accuracy of the experimental measurements can be found in.[7] The flow velocities were measured in the mid-plane, being also the symmetry plane, using particle image velocimetry (PIV) system by TSI Inc. (including the 120 mJ NewWave Solo Nd:YAG laser, 4096 x 2048 pixels CCD camera, Nikkor 60mm lens). About 2000 PIV snapshots were taken at the rate of 2 Hz and analyzed using the standard FFT-based cross-correlation algorithms using various commercial (Insight 3G, TSI Inc) and open-source software (OpenPIV , http://www.openpiv.net) for the verification purposes.

III. EXPERIMENTAL RESULTS AND DISCUSSION

All experimental results obtained in the present study were normalized using the scales L, U, $t=L/U$ for length, velocity and time, respectively. Thus, the only dimensionless parameter determining the flow in a cubical cavity is the Reynolds number defined as $Re=UL/\nu$, where ν is a kinematic viscosity. Note also that for the constant values of cavity length L and kinematic viscosity ν, the Reynolds number is varied only by a variation of the velocity, U. In the presented series of experiments we varied the

velocity of the lid to obtain the stable flow below (*Re* = 1480) and above (*Re* = 1970) critical point, predicted in our numerical study (Feldman and Gelfgat[6]).

Validation of the experimental results

Figure 2 illustrates a cross-verification of the experimental and numerical results in the sub-critical steady state regime, showing velocity distributions along two centerlines (x,0,0) and (0,y,0) at the cavity mid-plane cross section for *Re* = 1480.

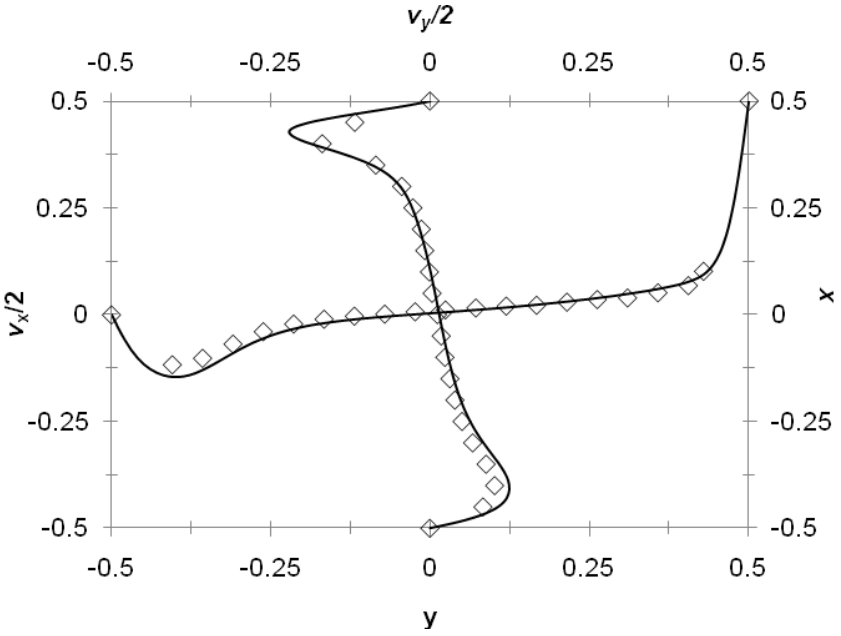

FIG.2.Comparison of the numerically (solid line) and experimentally (◊) obtained centerline velocities at the cavity mid-plane, *Re* = 1480.

A very good agreement is observed between the experimental and numerical results for the entire range of v_x and v_y velocity components with the exception of two narrow regions $-0.5 \le y \le -0.4$ and $0.4 \le y \le 0.5$ where the PIV measurements are not accurate enough, so that the corresponding points are not included in the figure. The experimental accuracy is limited near the reflecting surfaces. In spite of that, the experimental and the numerical v_y values are compared favorably in the vicinity of the cavity left and right walls.

Steady and non steady flow analysis

Following the numerical results of Feldman & Gelfgat[6], who investigated a set of sub- and slightly supercritical flows in a cubical lid-driven cavity, the steady – unsteady

transition occurs via subcritical Hopf bifurcation with $Re_{cr} \approx 1914$. It was also observed that at *Re* = 1970 the flow exhibits oscillations characterized by a dimensionless angular frequency ω=0.575 and its subsequent multiple harmonics. This fact motivated the next step of the present study at which a set of experiments have been performed for gradually increasing Reynolds numbers: *Re* =1480, 1700, 1970, 2100. It should be emphasized that because of the assumed sub-criticality of the Hopf bifurcation[6] the experiments should be performed in order of increasing *Re* numbers. When going between two adjacent *Re* numbers, the data acquisition for each *Re* started only after a sufficiently long time period (at least 500 turn-over times) necessary for the flow to reach asymptotic steady or oscillatory state. Figure 3 presents Fourier transform analysis of v_x component measured at the cavity mid-plane cross section in the control point (-0.325,-0.378,0) .

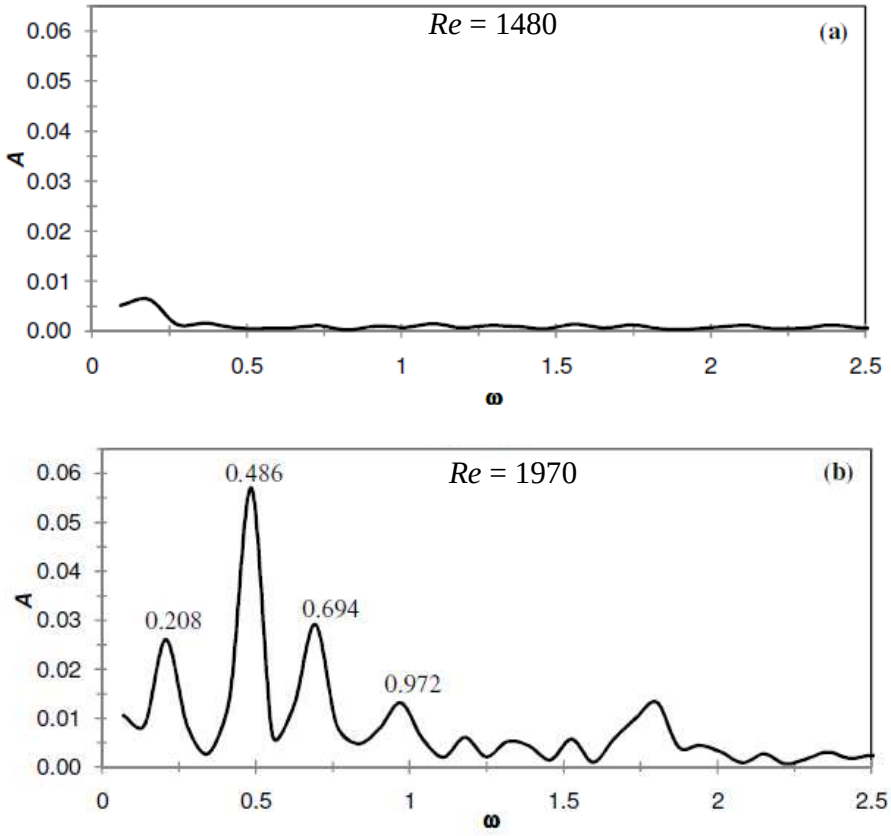

Fig. 3.Fourier transform of v_x velocity component measured at the control point (-0.325, -0.378, 0) located in the cavity mid-plane (z = 0) for: (a)-steady state flow, *Re* = 1480; (b)-unsteady flow, *Re* = 1970.

The control point is characterized by maximal amplitude of v_x oscillations observed numerically in the unsteady flow regime. As follows from Figure 3-a, at *Re* =1480 the frequency spectrum over the entire range of angular frequencies is flat with the close to zero amplitude, indicating on the steady state flow regime. The behavior at *Re* =1700 is similar, in agreement with the numerical results of Ref. 6 and not shown here for the sake of brevity. Further increase of Reynolds number to the value above the critical one, *Re* = 1970, led to a qualitatively different spectrum pattern containing discrete frequency spectrum with non-zero amplitude values corresponding to several non-decaying modes which determine unsteady oscillating flow inside the cavity (figure 3-b). These observations comprise a clear evidence for steady – unsteady transition taking place in the range of $1700 < \mathrm{Re} < 1970$. The angular frequency of the most unstable mode, corresponding to the largest amplitude, is $\omega = 0.486$. Note also that the leading mode is accompanied by its subsequent doubled harmonic $2\omega = 0.972$ whose presence is typical for non-linear dynamic systems. It should be noted that experimentally obtained angular frequency value of the most unstable mode differs by approximately 16% from that estimated numerically in Ref. 6. Along with the leading mode and its subsequent doubled harmonic there are also two additional modes whose influence on the cavity flow is significant. The modes are characterized by the angular frequency values equal to $\omega = 0.208$ and $\omega = 0.694$ which are close to 1/2 and 3/4 of the leading mode angular frequency. Note that the larger frequency $\omega = 0.694$ is just a superposition of the two lower ones, so that only the lowest frequency can be an independent harmonics. Unfortunately, the experimental sampling rate is too low to enable a definite conclusion here. We believe that appearance of the lower frequency is due to either a period-doubling or secondary Hopf bifurcation. The definite conclusion needs to be done by further experimental measurements allowing high resolution of the discrete frequency spectrum, which in the present work is restricted by the second decimal digit. The Fourier transform of v_x component performed for *Re* =2100 resulted in a wide dispersion of the angular frequencies indicating on appearance of continuous spectrum. This is an apparent nonlinear effect expected for the growing Reynolds number. The flow characteristics measured at *Re* =1970 are considered to be the closest to those of an instability onset predicted numerically.

For further comparison with the numerical results we filter out the main harmonics of oscillations using a standard band-pass filter. Figure 4 compares spatial distributions of v_x and v_y amplitudes at the cavity mid-plane computed and measured at *Re* =1970.

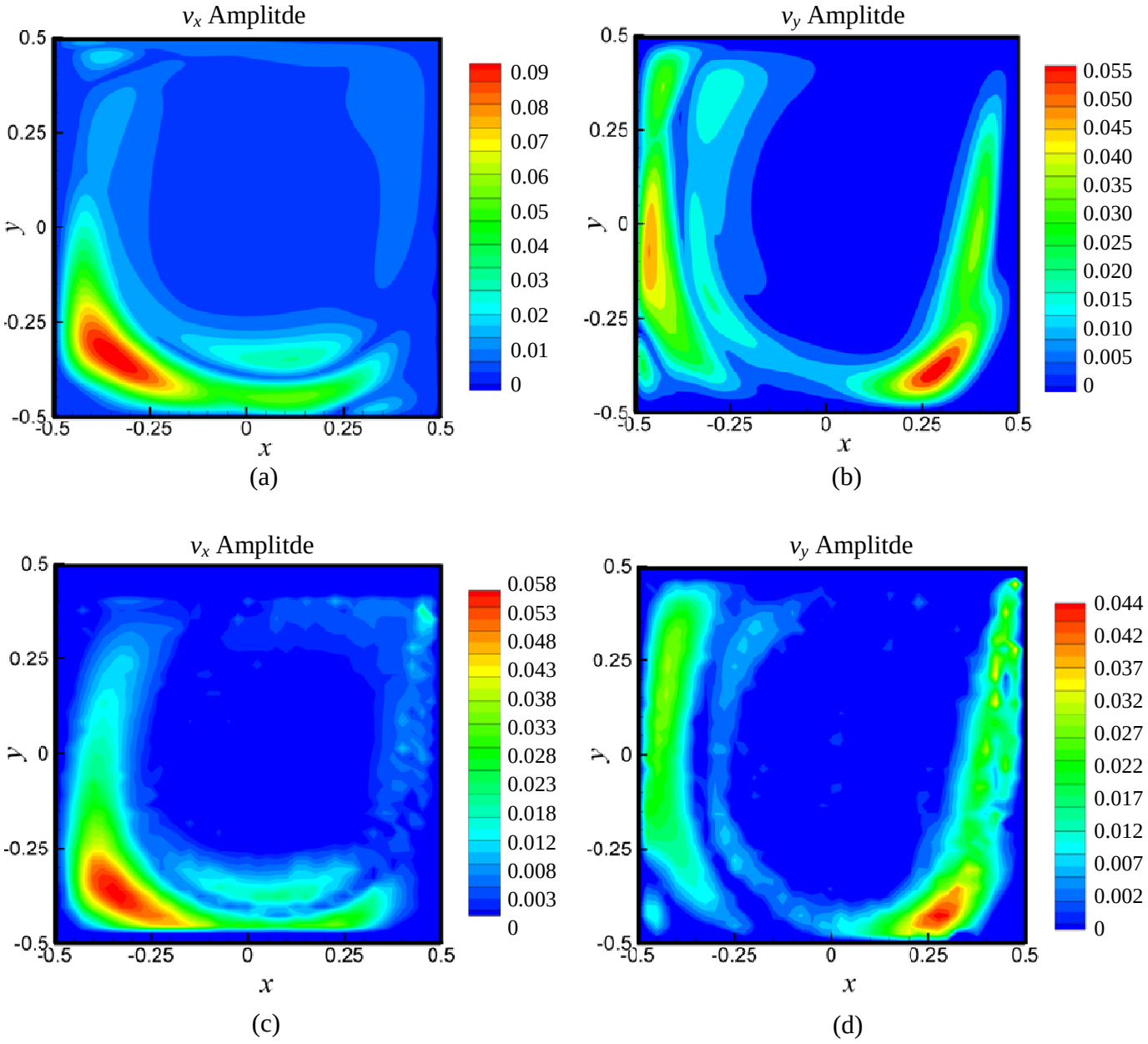

Figure 4. Spatial distributions of maximal v_x and v_y oscillation amplitudes at the cavity mid-plane, *Re* = 1970: (a)-(b) numerical results; (c)-(d) experimental results.

A good qualitative agreement between the numerical and the experimental spatial distributions for both amplitudes makes us confident of the fact that the same instability

has been computed and measured. As it has been already stated in Ref. 6 the maximum values of v_x and v_y oscillation amplitudes are located at the interface of the primary eddy with the secondary downstream and the secondary upstream eddies located respectively in the lower right and left corners of the mid plane cross section (see also figure 5). These numerical observations are in full agreement with experimental ones of the present study. The quantitative comparison reveals that the numerical values of v_x and v_y amplitudes are larger than the experimental ones. The maximum values of the measured v_x and v_y amplitudes comprise about 64% and 80%, respectively, from the corresponding computed values. This fact may be explained by existence of the energy dispersion intrinsic in the experimental set up in terms of undesirable vibrations of the moving lid and also induced by the measurement inaccuracies near the walls. The latter explains also the deviations between the numerical and the experimental spatial locations at which the maximal amplitude values of both velocity components are observed (see Table I).

	Maximal value of v_x Amplitude	Maximal value of v_y Amplitude
Numerical results	(–0.338,–0.343,0)	(0.289,–0.383,0)
Experimental results	(–0.325,–0.378,0)	(0.275,–0.427,0)

Table I. Comparison between locations of maximal values of velocity amplitudes obtained numerically experimentally.

The filtered flow field, containing only the most unstable mode and its subsequent doubled harmonic, is used also for a visualization of the 3D cavity flow. Figure 5–a presents a snapshot of the typical flow pattern at the cavity mid-plane at *Re* =1970 characterized by secondary upstream and secondary downstream eddies located in the left and right corners, respectively, and by a primary eddy located in the central part of the cavity. Figures 5b-5e show four velocity snapshots at the left and right corners of the mid-plane where the maximum values of velocity oscillations are observed. It is assumed that the latter, as well as the entire instability mechanism, is a result of interaction between the primary and the secondary eddies taking place at the boundary between them. The oscillating pattern of a slightly supercritical flow has been already described

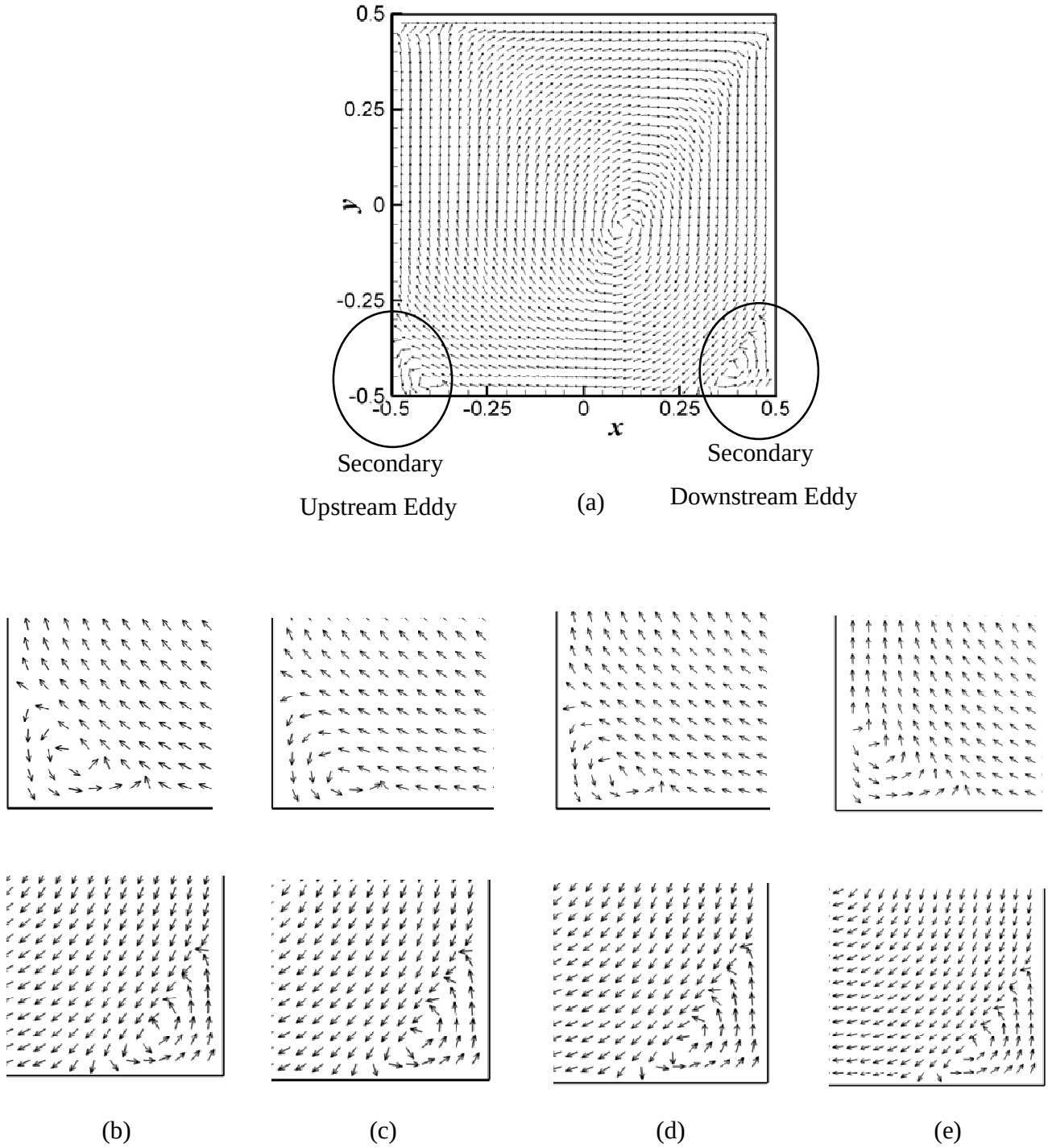

Fugure 5. Flow velocity vectors at the cavity mid-plane (*x*, *y*, 0) over a single period, *Re* = 1970 :(a) general view; (b)-(e) velocity snapshots of the secondary upstream and downstream eddies: (b) *t* = 0;(c) *t* = 3.23; (d) *t* = 6.46; (e) *t* = 9.7. The lid motion is indicated by the arrow (enhanced online).

numerically in Ref. 6. The snapshots in figure 5 are equally spaced in time over a single period. For the visualization purposes all velocity vectors are plotted with the uniform length independently of their numerical values. Because of the low precision of the flow

properties measured close to the cavity boundaries the velocity values in these regions were estimated by a linear interpolation between the corresponding boundary values, known from the non-slip boundary conditions, and the nearby measured interior velocity values.

IV. CONCLUSSIONS

An experimental study of a cubical lid driven cavity flow for a set of *Re* numbers corresponding to the steady and unsteady flow regimes has been performed. The study showed that the steady state is stable for $Re < 1700$ at least. The obtained experimental results have been then successfully compared with the corresponding numerical steady state solutions. It was found that a steady – unsteady transition occurs in the range $1700 < \mathrm{Re} < 1970$. Beyond $Re = 1970$ the flow becomes oscillatory with the dimensionless angular frequency of the main harmonics $\omega \approx 0.486$. Both, the location of the threshold and the oscillations frequency are in a good agreement with the numerical results of Ref. 6 where instability had been predicted at $Re_{cr} \approx 1914$ with $\omega \approx 0575$. The experimental pattern of the spatial distribution of the velocity amplitudes is in good qualitative agreement with that of the numerical solution, thus proving that both results address the same instability mode. Accurate quantitative measurement of the critical Reynolds number remains open and will comprise the scope of our future studies. Nevertheless, we believe that the accuracy of the present results is sufficient for the validation of the main result - experimental observation of the oscillatory instability at Reynolds numbers, which are lower than predicted in former experiments and rather close to the recently predicted value. Undoubtedly, further improvement of the experimental set up and a larger set of experiments, varying the size, velocity and the kinematic viscosity of the fluid, directed toward diminishing of the experimental uncertainties is still needed to gather the quantitative data for the primary and consequent transitions in three-dimensional lid-driven cavity flows.

Acknowledgement

This study was supported by German-Israeli foundation, grant No. I-954 -34.10/2007, and by the Israel Science Foundation, grant No. 782/08.

References

[1] P.N. Shankar, M.D. Deshpande, “Fluid Mechanics in the driven cavity,” Annual Review of Fluid Mechanics **32**, 93 (2000).

[2] V.Y.A. Bogatyrev, A.V. Gorin, “End effects in rectangular cavities,” Fluid Mech.-Soviet Res.**7**, 101 (1978).

[3] J.R. Koseff, R.L. Street, “On the endwall effects in a lid-driven cavity flow,” J. Fluids Eng. **106**, 385 (1984).

[4] R. Iwatsu, K Ishii, T. Kawamura, K. Kuwahara, J.M. Hyun, “Numerical simulation of three-dimensional flow structure in a driven cavity”, Fluid Dynamics Research **5**, 173 (1989).

[5] A.K. Prasad, J.R. Koseff, “Reynolds number and end-wall effects on a lid-driven cavity”, Phys. Fluids A **1**, 208 (1989).

[6] Yu. Feldman, A.Yu. Gelfgat, “Oscillatory instability of a 3D lid-driven flow in a cube,” Submitted to Phys. of Fluids

[7] M. Kreizer, D. Ratner, A. Liberzon, “Real-time image processing for particle tracking velocimetry,” Experiments in Fluids. **48:1**, 105 (2010).